Detection of active faults using data fusion techniques – Case study: Psachna - Island of Evoia, Greece

Chrysa C. Gountromichou[*a], Christine Pohl[**b]
[a]Earthquake Planning and Protection Organization (E.P.P.O.); [b]International Institute for Geo-Information Science and Earth Observation (ITC)

ABSTRACT

The identification of active faults (faults potentially capable to trigger an earthquake) is important for a seismically active country like Greece. Remote sensing techniques and GIS analysis were used in order to detect, map and characterize the tectonic structures of Psachna town and the surrounding area in central Evoia, Greece.

Geometrically corrected and processed Landsat ETM+ data are used for the lineament analysis. The expert knowledge for the interpretation of the lineaments was used against algorithm and other automatic methods in order to increase the qualitative accuracy of the method. The refined lineament map, the seismic data of about the last 40 years, the Quaternary formations map, and the drainage anomalies map were integrated in a GIS. The proposed model examines and classifies every lineament based on a set of predefined criteria. The classification system is in accordance with the official regulations for neotectonic mapping in Greece and consists of four classes: active fault, possible active fault, inactive fault and lineaments. Further analysis of the active and possible active faults shows two sets of directions, NW-SE and ENE-WSW striking. Both directions are in accordance with the extensional tectonic regime in the central Evoia in Pliocene and Middle – Upper Pleistocene, respectively.

Keywords: Data fusion, image processing, Landsat ETM+, neotectonics, active faults, seismicity, central Evoia, Greece.

1. INTRODUCTION

1.1 Geology - Neotectonics

Eastern central Greece is an actively deforming continental province, in the concave part of the Hellenic Arc and has been undergoing extension since early Pliocene (McKenzie, 1978). The extension is a combination of two effects: the on-going subduction, northwards, of an ancient remnant of ocean lithosphere along the Hellenic Trench, and an additional component of N-S extension (±20º), which is caused by the westward movement of the Anatolian block (Taymaz et al. 1991). Therefore, the geomorphology of central Greece is dominated by normal faults with an E-W to NW-SE strike.

The whole Gulf of Evoia is a graben with a total length of almost 100km that is bounded by normal faults (Roberts & Jackson, 1991). The study area is located at the northeastern side of the northern Gulf of Evoia. The extensional strain is accommodated by sets of normal faults, of planar geometry, moderate dips, and by clockwise rotation of upper crustal blocks (Jackson, 1994).

The study area mainly belongs to the Sub-Pelagonian zone, which is the western margin of the Kimmerian continent – Pelagonian zone- to Neo-Thythes sea, and only the eastern part is covered with the upthrusting formations belonging to the Pelagonian zone. Thus, the alpine basement consists mainly of carbonate rocks, like limestones, dolomites, and limestones with intercalation of dolomitic limestones, with different degree of karsticity, and thin to thick bedded layers (IGME, 1981).

The uplift of the area is marked with the presence of an undivided flysch, fine to medium-grained sandstones alternating with shales, Maastrichtian - Paleocene age. At the top of the stratigraphic sequence, there are Neogene and Quaternary sediments. The Neogene sediments are mainly lacustrine deposits with layers of conglomerates, marls, sandstones, clays and marly limestones. The Quaternary consists of the Pleistocene formation of lacustrine to brackish facies,

Remote Sensing for Environmental Monitoring, GIS Applications, and Geology II, Manfred Ehlers, Editor, Proceedings of SPIE Vol. 4886 (2003) © 2003 SPIE · 0277-786X/03/$15.00

weathered material from the surrounding rocks, recent and old cones of unconsolidated scree deposits, and alluvial deposits (IGME, 1981).

The recorded seismicity in the area shows moderate to low activity at the last 40 years of records. No earthquake greater than 5.0R is recorded. On the other hand, the historical seismicity is poor and is lacking detailed information, especially from the period 1800 and further back in time (Ambraseys 1978, Papazachos & Papazachou 1989, Ambraseys & Jackson 1990, Ambraseys 2000). Both statements seem to plead against the hazardous seismicity in the area. However, it must be taken under consideration that the lack of long-term observation in many regions in Greece states an apparent low earthquake hazard.

The whole study is based on the following definitions for the activity of the faults, which are in accordance with the standing regulations for neotectonic mapping in Greece: an active fault is defined as the fault that has been activated the last 10,000 years, in the Upper Pleistocene age; a possible active fault is the one, which has been triggered by an earthquake from Upper Pleiocene to Upper Pleistocene; and an inactive fault is a fault that has not been activated from the Lower Pleiocene and onwards.

2. METHODOLOGY

The methodology followed in this case study consists of:

a. Data processing - Image processing (image enhancement, appropriate filtering techniques, image fusion techniques) of the Landsat 7 ETM+ data (acquired on 21 June 2000 – path 183, row 33) producing the most refined lineament map.

b. Integration of multi - source spatial data, such as the produced lineament map, seismicity (1964-today), geological data in scale 1:50,000 (geological units, known faults), detailed drainage system and geomorphologic features in a Geographic Information System (GIS) based on predefined criteria.

c. Analysis and field check for verification of the data and construction of the final output: the neotectonic map.

Further statistical analysis to the faults has been carried out in order to understand their seismic behavior and their relation to each other and to the earthquakes. ERDAS IMAGINE V. 8.4 was used for the image processing and all the GIS analysis was completed using ILWIS V. 3.1 software.

2.1 Data processing

The data integration in a GIS requires some processing to all the input data. Moreover, the neotectonic mapping application itself requires high quality of the input data - maps in order to obtain a better product - the final map, since it contains spatial information about the active and possible active faults.

The processing of the geological map (scale 1: 50,000), map sheet "Psachna - Pilion" leads to four attribute maps concerning geological information: the Quaternary and the Neogene formations maps, the basement map (Fig. 1), and

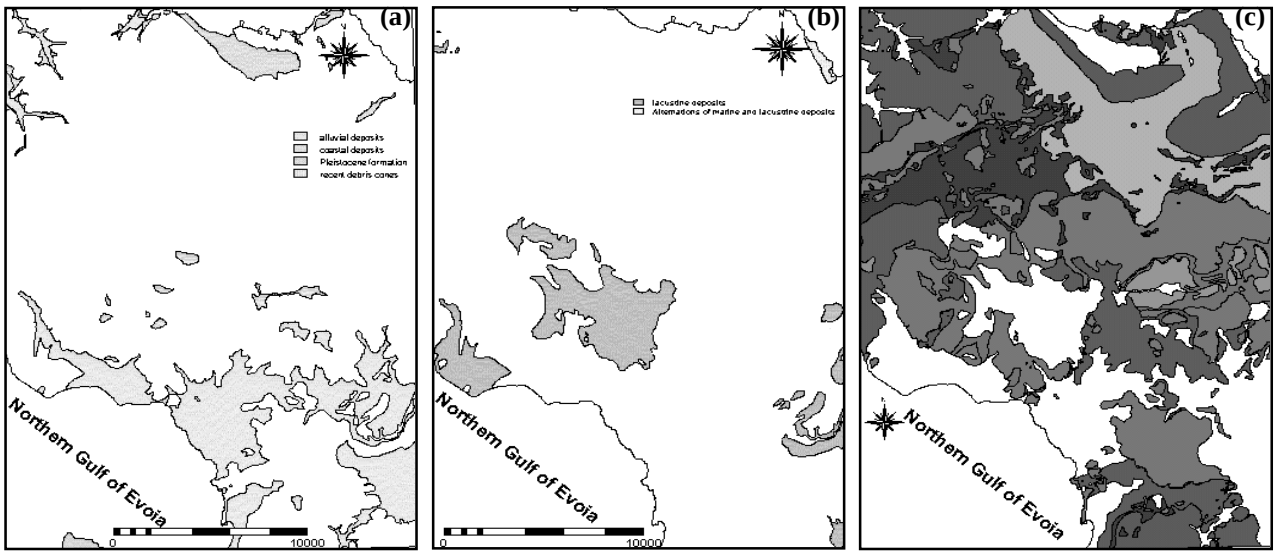

Fig. 1: (a) Quaternary formations map; (b) Neogene formations map; and (c) Basement map. All the maps derived from the geological map, Psachna - Pilion Sheet, scale 1:50,000 (IGME, 1981).

the known fault map.

The seismicity has been downloaded from the databases of the National Earthquake Information Center of the United States (U.S.G.S.) and of the National Observatory of Athens, Greece. The dataset from National Observatory of Athens, Greece was finally selected due to the completeness of the data. The 224 earthquakes in the last 38 years are plotted in a map and spatial pattern analysis of the seismic events is carried out indicating a cluster pattern, i.e. subgroups of epicenters tend to be significantly closer to each other. In addition, the fault map is buffered with a 500m distance in order to see whether or not earthquakes could be related to known faults (Fig. 2a).

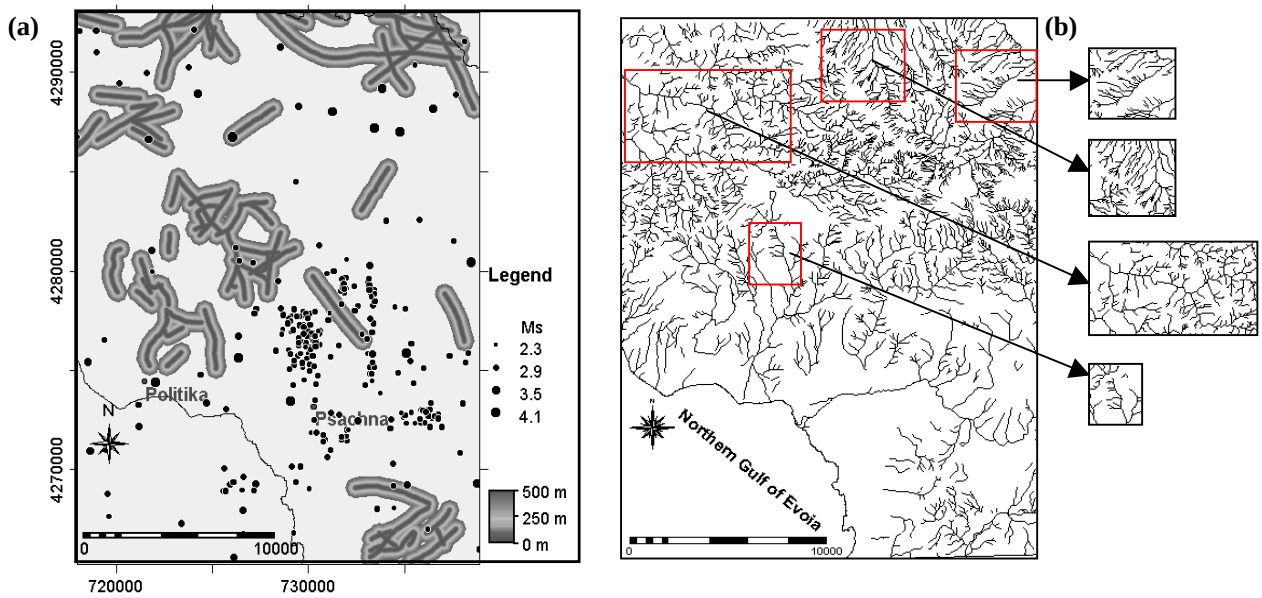

Fig. 2: (a) 500m buffered map of the known fault map as digitized from the geological map (1:50,000) together with the seismic epicenter of the earthquakes in the last 38 years in the area. (b) Drainage pattern of Psachna area digitized from the topographic map (scale 1:50,000). Areas with strong drainage anomalies controlled by tectonic structures are indicated in the boxes.

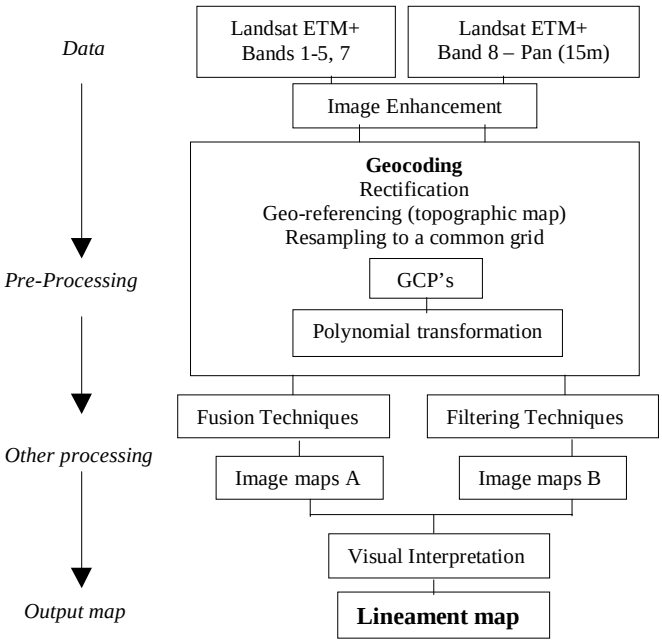

Fig. 3: Diagram for image processing for lineament analysis.

The drainage pattern was digitized from the topographic map (scale 1:50,000) in order to identify those areas where strong drainage anomalies are present (Fig. 2b). These areas are related to recent structural deformation (Doornkamp, 1986).

The most critical part of the data processing is the Landsat 7 ETM+ image processing which provides the lineaments to the system. The main steps in the image processing are shown in Fig. 3. The most interesting parts are the applied filtering techniques and the image fusion for lineament detection. The image was georeferenced to UTM zone 34 by a 1st order polynomial transformation selecting ground control points (GCP' s) from 1:50,000 recent topographic map (Hellenic Army Geographical Service, 1990). All these spatial data are referring to the same geographical system and have the same horizontal datum (UTM zone 34, WGS 84).

2.1.1 Filtering Techniques

Filtering techniques are the most popular for lineament identification and delineation (Terry et al. 1977, Carrere 1990, Süzen & Toprak 1998, Pradeep et al. 2000). Although, there have been significant approaches for the evaluation and automatic detection of the lineaments and curvilinear features from satellite images (Cross 1988, Karnieli et al. 1996), the human expertise is still an asset for lineament detection and interpretation with its subjective perception.

The experience has shown that the best interpretation is achieved with the use of the panchromatic band, which has high spatial resolution (15m). In order to obtain a better image for interpretation some processing with techniques, such as filtering techniques, histogram equalization, standard deviation stretching, should take place.

The produced lineament map is an "additive" product based on visual interpretation of lineaments. The concept is that every time the former lineament map is the basis for the following interpretation, which is taking place in different filtered image (Fig. 4). First, the panchromatic image is enhanced with the *histogram equalization method* where the interpretability has been improved and more discrete features are visible and then, a primary interpretation has taken place producing the lineament map 1.

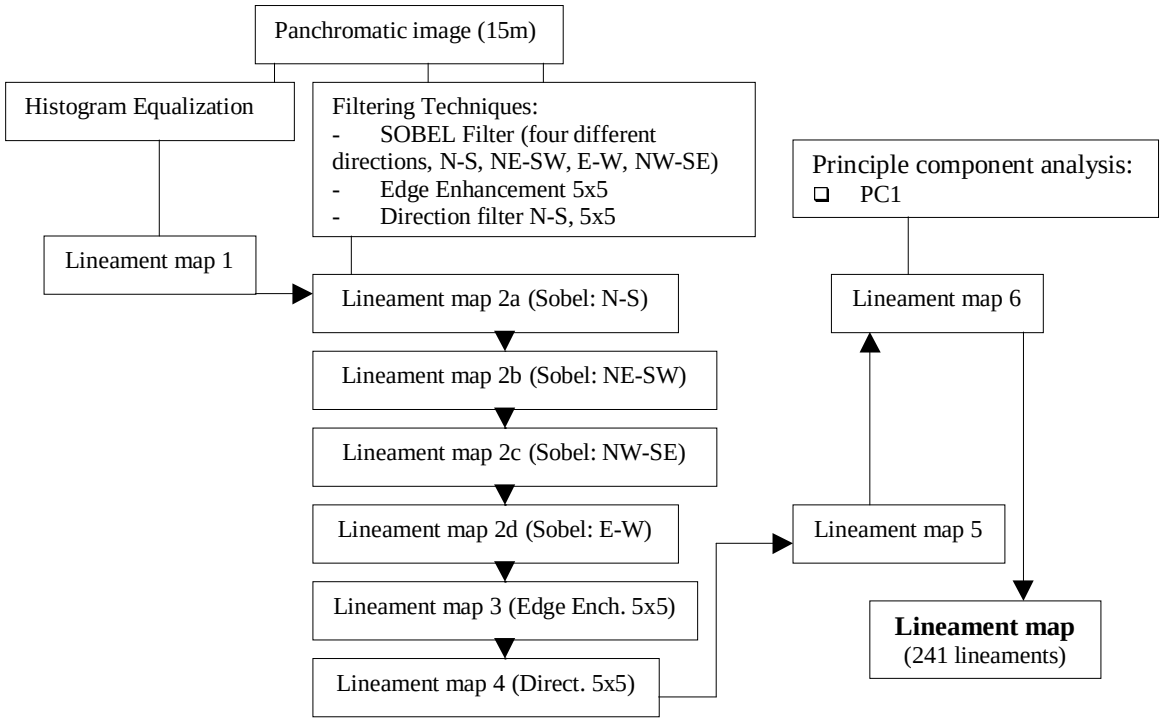

Fig. 4: Lineament map based on filtering techniques.

One of the most well-known filters in lineament analysis is the *Sobel directional filter* that usually is applied in two directions, here it has been run in the four directions, N-S, NE-SW, E-W, NW-SE (Fig. 5) (Süzen & Toprak, 1998) producing the intermediate maps, lineament map 2a – 2d. In this case, more emphasis was given to the NW-SE and N-S directions where the filters enhance the NE-SW lineaments and the E-W respectively, without excluding the visibility of the other directions. The reason is that the expected normal faults, which belong to the latest tectonic regime

(neotectonic faults), are formed due to the N-S and NW-SE composite extension in the area. Moreover, *edge enhancement* 5x5 kernel has been applied, which keeps the spatial information of the image (lineament map 3). In this paper, it is proposed another *run-once directional* 5x5 kernel (Fig. 6), which enhances by running it once, all the desired directions (lineament map 4). The convolution of these strong directional filters alter the appearance of the images (Fig. 7), thus to avoid this ambiguous appearance, the original band 8 is added to that in order to get back the spatial features and to continue with the lineament interpretation (lineament map 5). Last check of the lineament map is based on PC1 (lineament map 6). PC1 is a product of the Principle Component Analysis method (PCA), which is a commonly used technique for analysis of remotely sensed data. It has been used for data enhancement (Soha & Schwarz, 1978), as a data compression technique (Chavez & Kwarteng, 1989), to detect changes in land cover (Byrne et al., 1980) and also for merging multisensor data (Jutz & Chorowicz 1993, Yésou et al 1993). The use of only the PC1 is that this component contains the maximum information of all 8 TM bands to which the PCA has been applied. The refined lineament map contains 241 lineaments and is shown in Fig. 7 overlaid in a Sobel filtered image.

	N-S			NE- SW			E-W			NW-SE		
SOBEL	-1	0	1	-2	-1	0	-1	-2	-1	0	1	2
	-2	0	2	-1	0	1	0	0	0	-1	0	1
	-1	0	1	0	1	2	1	2	1	-2	-1	0

Fig. 5: Sobel filters in N-S, NE-SW, E-W, NW-SE directions.

Edge Enhancement 5x5				
-1	-1	-1	-1	-1
-1	-1	-1	-1	-1
-1	-1	49	-1	-1
-1	-1	-1	-1	-1
-1	-1	-1	-1	-1

Run - Once Directional filter 5x5				
-1	-1	0	1	1
-1	-2	0	2	1
-2	-2	0	2	2
-1	-2	0	2	1
-1	-1	0	1	1

Fig. 6: Edge enhancement 5x5 filter and the run - once directional filter 5x5 that enhance the NW-SE, E-W, and the NE-SW directions.

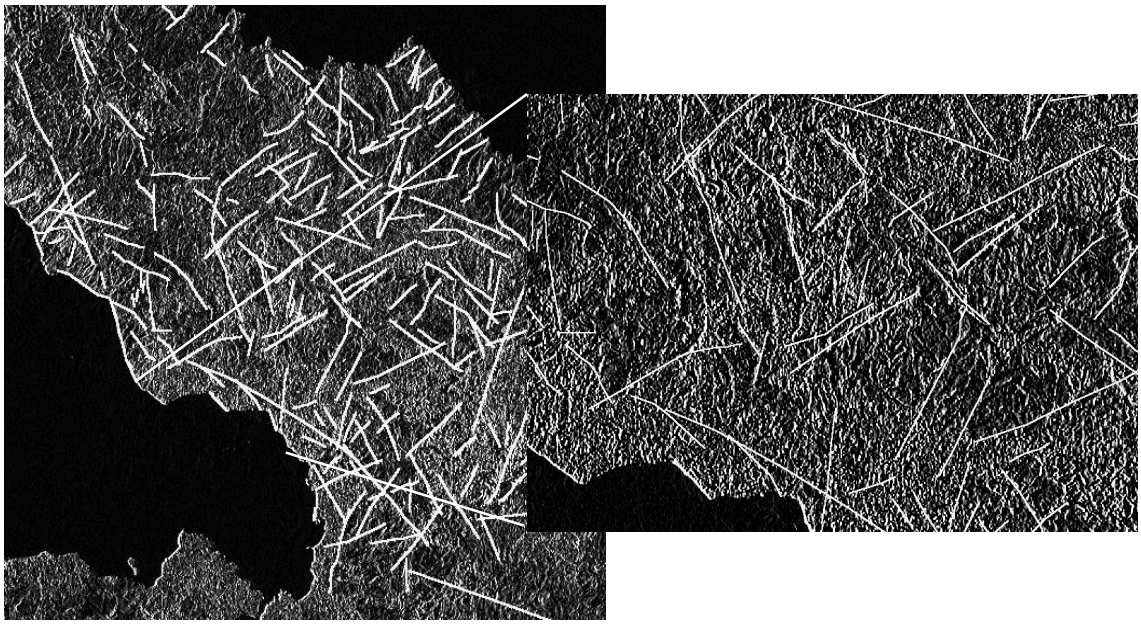

Fig. 7: Sobel filtered image (band 8) overlaid by the refined lineament map and a zoom area to the right side.

2.1.2 Fusion Techniques

In accordance to the most recent approaches there is an agreement that image fusion is certainly a framework and not just a single tool that is applied in any case. According to Wald, 1998, "Data fusion is a formal framework in which are expressed means and tools for the alliance of data originating from different sources, in order to obtain information of grater quality". A general definition for image fusion is given as the combination of two or more different images to form a new image by using a certain algorithm (van Genderen and Pohl, 1994).

For the current study, image fusion has been used as a tool to obtain the maximum information of a single sensor in one image and thus, to improve the interpretability for lineament analysis. The aim is to merge the spatial resolution of the panchromatic image preserving the spectral resolution of the multi-spectral TM images. Therefore, the fusion has been performed in a single sensor – spatial type of data set, i.e. same sensor, Landsat 7 ETM+ and different spatial resolution, high/low resolution (Pohl and van Genderen, 1998). Studies of this type of data are known for panchromatic and multi-spectral SPOT (Cliché et al. 1985). The methods applied for improving significantly the interpretability and the sharpening of optical data are colour related techniques (RGB, and IHS) and statistical and numerical methods (Brovey Transform) (Pohl and van Genderen, 1999).

According to Yésou *et al.* 1993, the optimum dataset for RGB combination can be determined empirically or statistically. The empirical approach is based mainly on the *a priori* knowledge of the spectral properties and on the application. The best discriminative sets for geological applications, in decreasing order, are TM 542, TM 743, TM 543 and TM 752. The TM 542 combination allows the best perception of the geological structures and the most contrasted color composite is obtained with the (R,G,B)=(2,5,4) (Fig. 8). Another interesting combination is TM 843, which integrates the higher spatial resolution of band 8, provides natural colors to the image and improves the interpretability of the geological features. Both RGB combinations are presenting interesting results and are highly recommended for geological applications.

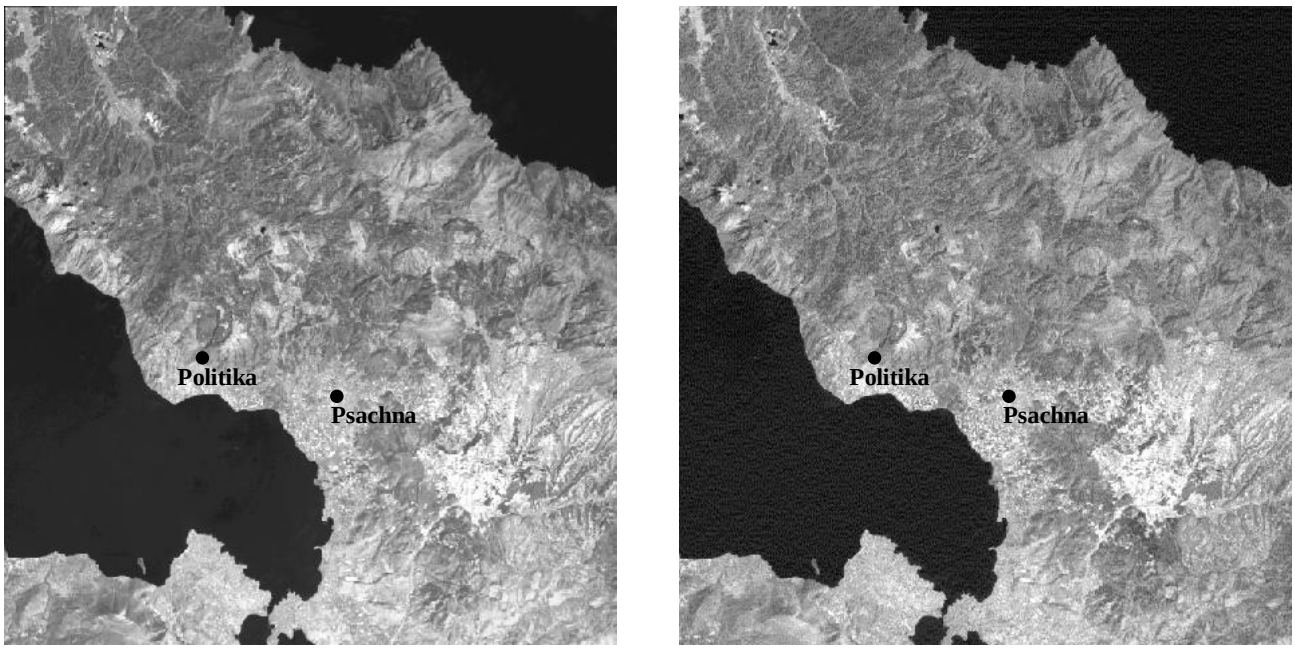

Fig. 8: The (R,G,B)=(2,5,4) combination appropriate for neotectonic mapping (left image). Brovey Transform applied to (R,G,B)=(2,5,4) with the panchromatic band 8 (right image).

The IHS has been used to enhance highly correlated data (Kaufmann, 1988), but also for geological features enhancement (Daily 1983, Yésou et al. 1993). For this case study, the IHS transform has used the method where the Intensity for the selected (R,G,B)=(2,5,4) combination is being replaced by the band with the higher resolution, the panchromatic band of the Landsat 7 ETM+ data and the reverse transform to RGB is achieved. The spatial resolution in the IHS image is well merged, but the spectral resolution of the TM bands has been diminished. (R,G,B)=(2,5,4) band combination was used for the Brovey transform as well, in order to sharp the image and preserve the spectral integrity

of the data (Pohl and van Genderen, 1999). The Brovey image enhances the drainage pattern and gives the relief impression (Fig. 8), which are helpful for the lineament identification. The combination of filtering and fusion techniques provides the final lineament map, which contains 258 lineaments.

3. DATA PROCESSING AND DATA INTEGRATION IN A GIS

3.1 Integration of the multi - source data in a GIS

Spatial data analysis in a GIS is the process of seeking patterns and associations on maps that help to characterize, understand and predict spatial phenomena. Classification is a method for simplifying complex phenomena, and is used in a GIS for generalization and enhancement. It means either the process of assigning objects to classes on the basis of one or more attributes, or the process of defining multivariate classes, or for a single attribute the list of breakpoint values that define class intervals (G. F. Bonham-Carter, 1994).

The model used in the neotectonic mapping application involves finding those lineaments that satisfy a set of predefined criteria – conditional statements. The criteria are defined as a set of deterministic rules, the model consists of applying Boolean operators to a set of input maps and the final output is a composite map, which contains the information of three binary maps, the active fault map, the possible active fault map and the inactive fault map.

Map Name	Description	Source
Lineam	Final lineament map	Advanced processed Landsat 7 ETM+ images
Quater	Quaternary formations (polygon map)	Digitized from Geological map (1: 50,000)
PreQuater	Pre Quaternary formations (polygon map)	Digitized from Geological map (1: 50,000)
Fault	Known normal faults (segment map)	Traces digitized from Geological map (1: 50,000) and buffered
Seism	Epicenters of the seismic events from 1964-2002 (point map)	Tabular data from National Observatory of Athens
Drain	Drainage anomalies (segment map)	Extracted from the drainage pattern, which has been digitized from the topographic map (1: 50,000)

Table 1: Maps used for neotectonic mapping example, Pschna area, Island of Evoia, Central Greece.

The criteria are based on the following maps:

– *The Quaternary formations map*: Lineaments that are located within Quaternary formations, and especially they mark a linear contact between the young Quaternary formations and the alpine basement, are most probable active neotectonic structures (Steward & Hancock, 1993).

– *The PreQuaternary formation map*: Lineaments within PreQuaternary formations have low probabilities to be considered as possible active faults unless there is a seismic event related to fault otherwise is characterized as inactive fault by the system.

– *The known fault map*: It contains all the already mapped normal faults in the study area. This map is used for finding the relation between a lineament and a fault, i.e. if a lineament coincides or not with a known fault, or it is as an extension or a part of the fault. For obtaining better understanding of the distances between the lineaments and the faults, a 500m buffer zone has been created to the fault map.

– *The epicenters of the seismic events of the period 1964-2002*: The seismic data have been obtained from the Institute of Geodynamics, National Observatory of Athens and have been plotted in a point map. An attempt has been made to correlate these events according to their distance with the corresponding faults and lineaments. Buffered maps of a distance 500m are used.

– *The drainage anomalies map*: It consists of all the anomalies of the drainage pattern and is used as a strong evidence of tectonic activity in the area. When a lineament is following a strong drainage anomaly means that there is a weak zone, most probable a tectonic discontinuity.

All the aforementioned criteria – maps are used to determine the criteria - conditional statements that are appropriate for neotectonic mapping. The basic concept of the analysis in order the system to classify lineaments as active, possible active and inactive faults is based on those conditional statements.

A lineament can be considered as active fault when it fulfills the following conditional statements:

1. There is a seismic event within a 500m distance AND,
2. Coincide with a known fault, OR is parallel to a known fault, OR is an extension of a known fault, OR is a part of it AND,
3. Is located in Quaternary formations, OR is a boundary between Quaternary formations and the alpine basement, AND,
4. Corresponds to a strong drainage anomaly.

As possible active fault:

1. There is a seismic event within a 500m distance AND,
2. Coincide with a known fault, OR is parallel to a known fault, OR is an extension of a known fault, OR is a part of it OR,
3. Is located in Quaternary formations, OR is a boundary between Quaternary formations and the alpine basement, OR,
4. Corresponds to a strong drainage anomaly.

As inactive fault:

1. There is a seismic event within a 500m distance OR,
2. Coincide with a known fault, OR is parallel to a known fault, OR is an extension of a known fault, OR is a part of it OR,
3. Is located in Quaternary formations, OR is a boundary between Quaternary formations and the alpine basement, OR,
4. Corresponds to a strong drainage anomaly.

The appropriate class has been assigned only to those lineaments where the aforementioned conditional statements were met; the rest lineaments remained as unclassified lineaments. The final refinement for the verification and classification of the lineaments has taken place after the fieldwork. According to the standing regulations for neotectonic mapping the final output must contain the information from remotely sensed data, in addition to the verified in the field faults. Thus, the final output is a map that consists of four classes, containing the lineaments as well (Fig. 9).

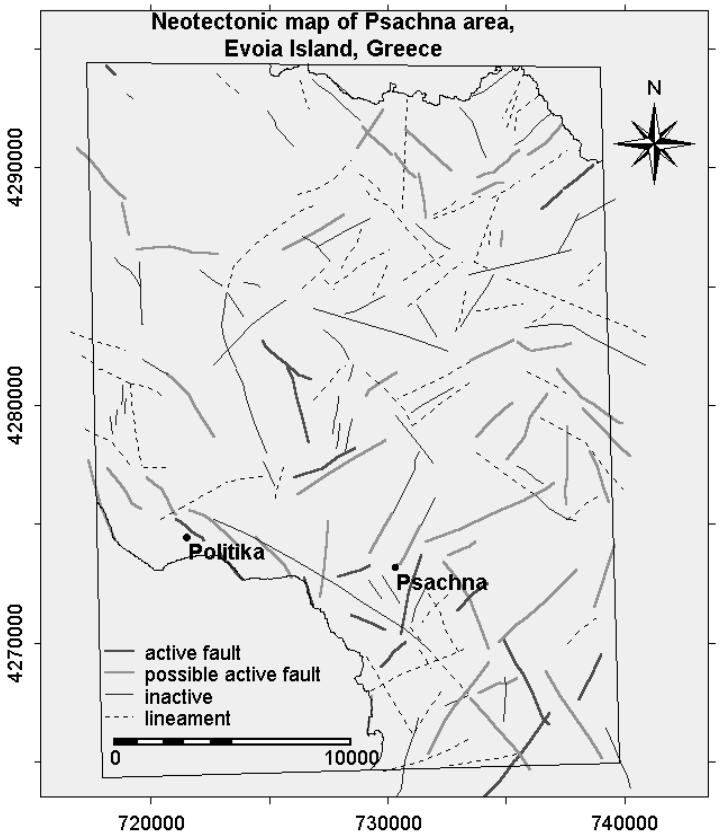

Fig. 9: Final output, the neotectonic map of the area.

4. RESULTS

This work provides interesting results related to the tectonic activity, the main geological structures, and the characteristics of the faults in the study area. It determines the methodological framework of image fusion and data integration as most appropriate for extracting all the required spectral and spatial characteristics referring to the identification of active faults.

The earthquakes for the period 1964-2002 are characterized as shallow with a depth less than 10km and a magnitude, which ranges between 2.4 and 4.2R (Fig. 10a). Although the database does not contain data of very low magnitude (<2.4R) their frequency is relatively high, since in the last 38 years at least 224 events have been recorded (average 1 earthquake every 2 months).

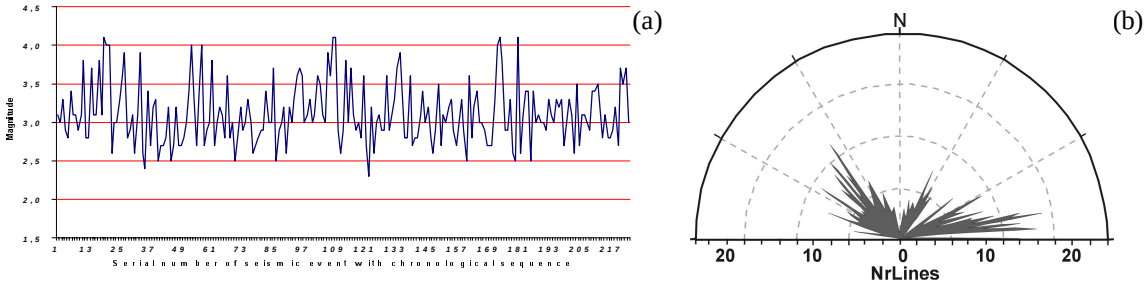

Fig. 10: (a) Chronological representation of the seismicity in the area of Psachna for the last 38 years (1964-2002. Shallow earthquakes with a range of magnitude between 2.4-4.2R. (b) Rose diagram of the active and possible active faults.

The fieldwork confirms the fact that some of the active and possible active faults from the final output map belong to the same fault zone system and are in a relation to each other. The active parts are segments of longer tectonic structures (de Polo et al., 1989) and in some cases their continuation is a possible active or an inactive fault.

Statistical analysis is also carried out for the active and possible active faults in the area in order to understand any relation to each other, as well as the main directions of the neotectonic structures. Thus, the rose diagram shows two predominant sets of directions (Fig. 10b), the NW-SE and the ENE-WSW. Since the structures have normal sense of movement, they belong to the youngest N - S extension tectonic regime.

Another statistical approach is referring to the relation of the lineaments with the known faults and the geology. Both factors are equally important in order to understand the relation of the lineaments with data set derived from the geological map (Quaternary formation map, Pre-Quaternary map, and known fault map). The pie-diagram 1 shows that the highest percentage belongs to the class: "lineaments within the basement". This class does not mean that these lineaments could not be considered as neotectonic faults, but there is lower probability to be such, than lineaments in Quaternary formations. On the other hand, a lineament that marks the boundary between the basement and the recent formations has higher probability to be a neotectonic fault and in particular an active fault. The relation of the lineaments with known faults is determined by three classes: lineaments that coincide with known faults, lineaments as extension and lineaments parallel of known faults (in total 13 %). Looking only at the relation of the lineaments with known faults and the geology, 5% could not be classified in one of the categories mentioned above, because there was no relation with the known faults and the

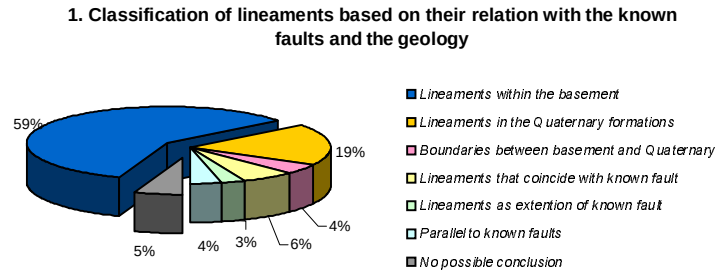

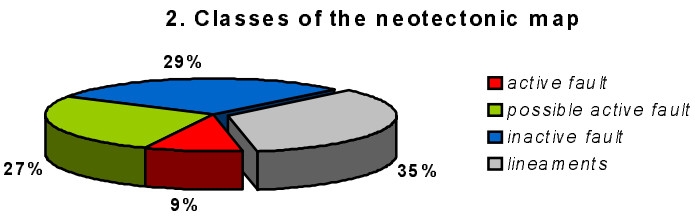

geological information is mixed. 6% of the total lineaments coincide with the known faults. Considering the peculiar cases of lineaments, which are very probable to be classified as faults (the sum of the light color pies in the pie-diagram 1), the percentage is increasing to 36%.

Statistical analysis of the final output map, the neotectonic map, demonstrates that 9% of the detected faults are active and 27% are possible active faults. In other words, 36% of the identified faults have been activated at least one time from the Upper Pleiocene and onwards, and they consider to have the highest probability to be reactivated (pie diagram 2).

The combination of filtering techniques and image fusion is essential for neotectonic applications because it improves greatly the interpretability of the images and thus, more accurate lineament analysis is possible. Lines representing artifacts are excluded from the analysis and further study could be more effective. For example, in the area between Psachna town and Politika village, there is a belt-conveyer for industrial purposes, which looks like a lineament at the initial stages of the interpretation of the images, but becomes obvious that it is not such, in the fused images. In addition, the use of a GIS as tool for lineament classification based on pre-defined criteria is proved to be determinant of neotectonic mapping.

Multi-sensor remotely sensed data, such as aerial photography, SPOT imagery, might improve more the interpretation for lineament analysis and consequently help more to the neotectonic mapping. The higher the spatial resolution of the data, the better the accuracy of the geometric correction. In the case of the SPOT images or the aerial photography it could be possible to utilize the stereo capabilities in order to define the sense of movement of a fault and study other characteristics (geometry – length, segment boundaries, associations with tectonic landforms, etc). In addition, a shaded relief Digital Elevation Model (DEM) could be useful for the quantitative approach of the activity of the faults – segments (morphotectonic analysis, estimation of the displacement, erosion rate versus uplift rate, etc). Moreover, a detailed DEM may provide more accurate GCP' s for the geometric model.

5. CONCLUSIONS

In conclusion, the use of processed Landsat ETM+ images in combination with integration of multi source data in a GIS is effective, because the cover area of these images is appropriate for geological applications, such as the neotectonic mapping. The main aim of the research was the production of the neotectonic map of the Psachna area using the latest satellite images and a number of additional input data. This aim was achieved and the final neotectonic map increased the understanding of the tectonism of the area.

The use of remote sensing, including image pre-processing, fusion and filtering techniques, for the detection of lineaments is essential. The output of image processing has to be integrated with other input data (criteria) in a GIS, in order to be classified, and finally the neotectonic map to be produced.

Some of the major conclusions of this study are mentioned below:

– The recorded earthquakes in the area are characterized as shallow and low magnitude earthquakes, meaning that the epicenter is relatively close to the surface, and thus could not be very far from the activated fault.

– The final lineament map, as it is produced from the filtered images and has been confirmed by the fused images, is the most refined. The combination of filtering techniques with image fusion is proposed as an asset to neotectonic studies.

– The fieldwork is an essential part for a complete neotectonic study and for the verification of every structure. Although, the use of satellite imagery and GIS analysis are very powerful tools for identification of lineaments and their characterisation in a GIS model as active, possible active or inactive structures, it is still complementary.

– The spatial distribution of the active and the possible active faults indicates that recent tectonic activity is concentrated in the south-western part of the study area, almost parallel to the coastal line. This statement is in accordance with the existence of a tectonic graben in the North Gulf of Evoia. In addition, the statistical analysis of these faults provides two sets of directions, one NW-SE striking and the other ENE-WSW in accordance with the extensional tectonic regime in the central part of Evoia island in Pliocene and Middle - Upper Quaternary age, respectively.

– Most of the active and possible active faults in the study area represent reactivated segments of larger faults.

ACKNOWLEDGMENTS

A lot of people have contributed in the successful completion of this study. In particular many thanks:

Dr. P.M. van Dijk and Dr. T. Woldai for their support and useful comments especially in the geological part of the study. Mr. B. Maathius for his interest at the initial stage of the data processing and Dr. A. Ganas who supplied the Landsat ETM+ images from the archive of IIS SA.

REFERENCES

1. N. N. Ambraseys, "Middle East – A reappraisal of seismicity", *Q. J. Eng. Geol*, **11**, pp. 19-32. 1978.
2. N. N. Ambraseys, and J. A. Jackson, "Seismicity and associated strain of central Greece between 1890 and 1988", *Geophs. J. Int.*, **101**, pp. 663-708, 1990.
3. N. N. Ambraseys, "Material for Investigation of the Seismicity of Central Greece", *EC project "Review of Historical Seismicity in Europe" (RHISE)* 1989-1993. Source: http://www.globalnet.gr/seismoi_k_ell.html (19.08.02).
4. G. F. Bonham-Carter, Geographic Information System for Geoscientists: Modelling with GIS, Pergamon, pp. 398 1994.
5. G. F. Byrne, P. F. Crapper, and K. K. Mayo, "Monitoring land- cover change by principal component analysis of multitemporal Landsat data", *Rem. Sens. of Environ*., **10**, pp. 175-184, 1980.
6. V. Carrere, "Development of multiple source data processing for structural analysis at a Regional scale", *Photogr. Eng. and Rem. Sens.*, **56** (5), pp. 587-595, 1990.
7. P. S. Chavez, and A. Y. Kwarteng, "Extracting spectral contrast in Landsat Thematic Mapper image using selective principle component analysis", *Photogr., Eng. and Rem. Sens.*, **55** (3), pp. 339-348, 1989.
8. G. Cliché, F. Bonn, and P. Teillet, "Integration of the SPOT Pan channel into its multispectral mode for image sharpness enhancement". *Photogr. Eng. and Rem. Sens.*, **51**, pp. 311-316, 1985.
9. A. M. Cross, "Detection of circular geological features using the Hough Transform", *Int. J. of Rem. Sens.*, **9**, pp. 1519-1528, 1988.
10. M. Daily, "Hue – Saturation – Intensity split – spectrum processing of SEASAT radar imagery", *Photogr. Engin. and Rem. Sens.*, **49** (3), pp. 349-355, 1983.
11. C. M. de Polo, D. G. Clark, D. B. Slemmons, and W. H. Aymard, "Historical Basin and Range Province surface faulting and fault segmentation", In: Workshop on Fault Segmentation and Controls on Rupture Initiation and Termination (edited by Schwartz, D. P. and Sibson, R. H.), *U.S. geol. Surv. Open-File Rep.*, **89**-315, pp. 131-162, 1989.
12. J. C. Doornkamp, "Geomorphological approaches to study of neotectonics", *J. Geol. Soc. of Lond.*, **143**, pp. 335-342, 1986.
13. ERDAS IMAGINE®, Version 8.4, ERDAS INC, Atlanta Georgia, USA, 1999.
14. J. L. van Genderen, and C. Pohl, "Image fusion: Issues, techniques and applications. Intelligent Image Fusion", *Proceedings EARSeL Workshop, Strasbourg, France*, Sep. 1994, edited by J. L. van Genderen and V. Cappellini (Enschede: ITC), **11**, pp. 18-26, 1994.
15. HAGS (Hellenic Army Geographic Service), 1:50,000 topographic map "Psachna Sheet", 1990.
16. IGME, Geological map of Greece, Sheet Psachna, Scale 1:50.000, Athens, 1981.
17. ILWIS, Version 2.23, International Institute for Aerospace Surveys and Earth Sciences (ITC), Enschede, The Netherlands, 1999.
18. J. A. Jackson, "Active tectonics of the Aegean region", *Annual Reviews of Earth and Planetary Science*, **22**, pp. 239-271, 1994.
19. S. L. Jutz, and J. Chorowicz, "Geological mapping and detection of oblique extensional structures in the Kenyan Rife Valley with a SPOT/Landsat-TM datamerge", *Int. J. of Rem. Sens.*, **14**.(9), pp. 1677-1688, 1993.
20. A. Karnieli, A. Meiseis, L. Fisher, and Y. Arkin, "Automatic extraction and evolution of geological linear features from digital remote sensing data using a Hough Transform", *Photogr. Engin. and Rem. Sens.*, **62**, pp. 525-531, 1996.
21. H. Kaufmannm, "Mineral exploration along the Aqaba – Levant structure by luse of TM data. Concepts, processing and results", *Int. J. of Rem. Sens.*, **9** (10), pp. 1639-1658, 1988.
22. D. P. McKenzie, "Active tectonics of the Alpine-Himalayan belt: the Aegean Sea and surrounding region", *Geoph. J. of the Royal Astronomical Soc*. **55**, pp. 217-254, 1978.

23. National Earthquake Information Center, Earthquake database, U.S.G.S., USA, Source: http://wwwneic.cr.usgs.gov/neis/epic/database.html (01.07.02).
24. National Observatory of Athens, Seismicity of Greece, Earthquake database of Greece, Source: http://www.gein.noa.gr/Greek/home-gr.html (1.7.02).
25. B. Papazachos, and K. Papazachou, "The earthquakes of Greece", p. 356, *Ziti Editions*, Thessaloniki, 1989.
26. C. Pohl, "Geometric aspects of multisensor image fusion for topographic map updating in humid tropics", p.160, *ITC*, Publ. No 39. ISBN 90 6164 1217, 1996.
27. C. Pohl, and J. L. van Genderen, "Multi-sensor image maps from SPOT, ERS and JERS", *Geocarto. Intern.*, **14** (2), pp. 33-40, 1999.
28. C. Pohl, and J. L. van Genderen, "Multisensor image fusion in remote sensing: concepts, methods, and applications", Review article, *Int. J. of Rem. Sens.*, **19** (5), pp. 823-854, 1998.
29. K. S. Pradeep, K. Sandeep, and P. S. Ramesh, "Neotectonic study of Ganga and Yamuna tear faults, NW Himalaya, using remote sensing and GIS", *Int. J. of Rem. Sens.*, **21**(3), pp. 499-518, 2000.
30. S. Roberts, and J. A. Jackson, "Active normal faulting in Central Greece: an overview", The Geology of Normal Faults, *Geol. Soc. of London*, Special Publication, **56**, pp.125-142, 1991.
31. J. M. Soha, and A. A. Schwarz, "Multispectral histogram normalization", *Proc. 5e Symposioum Candien de Télédétection*, pp. 86-93, 1978.
32. I. S. Stewart, and P. L. Hancock, Active Tectonics, *Neotectonics*, ch. **18**, pp. 370-409, 1993.
33. M. L. Süzen, and V. Toprak, "Filtering of satellite images in geological lineament analysis: an application to a fault zone in Central Turkey", *Int. J. of Rem. Sens.*, **19**, 6, pp. 1101-1114, 1998.
34. D. P. Taymaz, J. A. Jackson, and D. McKenzie, "Active Tectonics of the North and Central Aegean Sea", *Geoph. J. Int.*, **106**, pp. 433-490, 1991.
35. W. O. Terry, A. A. Elsa, R. G. Alan, and O. L. Sabino, "Structure mapping on enhanced Landsat images of southern Brasil: Tectonic control of mineralization and speculations on metallogeny", *Geophysics*, **42**(3), pp. 482-500, 1977.
36. L. Wald, "Data fusion: a conceptual approach for an efficient exploitation of remote sending images", *Proc. Fusion of Earth Data, Sophia Antipolis, France*, pp. 17-22, 1998.
37. H. Yésou, Y. Besnus, and J. Rolet, "Extraction of spectral information from Landsat TM and merge with panchromatic imagery – a contribution to the study of geological structures", *Photogr. and Rem. Sens.*, **48** (5), pp. 23-36. 1993.
38. H. Yésou, Y. Besnus, J. Rolet, J. C. Pion, and A. Aing, "Merging Seasat and SPOT imagery for the study of geological structure in a temperate agricultural region", *Rem. Sens. of Environ*., **43** (3), pp. 265-279, 1993.

* cgountro@geo.auth.gr; phone 30 10 6728000; fax 30 10 6779561; http://www.oasp.gr; Earthquake Planning and Protection Organization (E.P.P.O.), 32 Xanthou St., GR-154 51, Athens, Greece; **pohl@itc.nl; phone 31 53 4874487; fax 31 53 4874336; http://www.itc.nl; International Institute for Geo-Information Science and Earth Observation (ITC), P.O. Box 6, 75 00 AA Enschede, The Netherlands.